AD-A166 631 THE EFFECT OF SMOOTHING THE DOPPLER RADAR DERIVED WIND FIELD ON PERTURBAT.. (U) AIR FORCE INST OF TECH WRIGHT-PATTERSON AFB OH G P ROSSER MAY 86 1/1

UNCLASSIFIED AFIT/CI/NR-86-31T F/G 4/2 NL

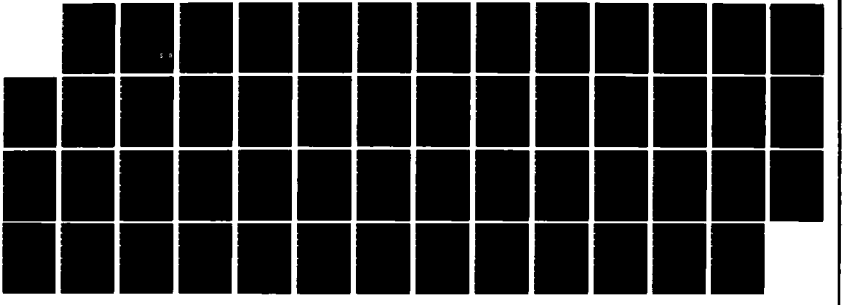

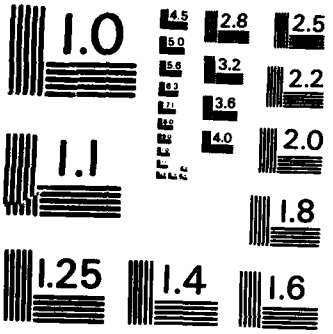

SECURITY CLASSIFICATION OF THIS PAGE (When Data Entered)

# REPORT DOCUMENTATION PAGE

READ INSTRUCTIONS BEFORE COMPLETING FORM

| | |
|---|---|
| 1. REPORT NUMBER: AFIT/CI/NR 86-31T | 2. GOVT ACCESSION NO |
| 3. RECIPIENT'S CATALOG NUMBER | |
| 4. TITLE (and Subtitle): The Effect of Smoothing the Doppler Radar Derived Wind Field on Perturbation Pressure Retrieval. | 5. TYPE OF REPORT & PERIOD COVERED: THESIS/DISSERTATION |
| | 6. PERFORMING ORG. REPORT NUMBER |
| 7. AUTHOR(s): George P. Rosser, Jr. | 8. CONTRACT OR GRANT NUMBER(s) |
| 9. PERFORMING ORGANIZATION NAME AND ADDRESS: AFIT STUDENT AT: Texas A&M University | 10. PROGRAM ELEMENT, PROJECT, TASK AREA & WORK UNIT NUMBERS |
| 11. CONTROLLING OFFICE NAME AND ADDRESS: AFIT/NR WPAFB OH 45433-6583 | 12. REPORT DATE: 1986 |
| | 13. NUMBER OF PAGES: 41 |
| 14. MONITORING AGENCY NAME & ADDRESS (if different from Controlling Office) | 15. SECURITY CLASS. (of this report): UNCLASS |
| | 15a. DECLASSIFICATION/DOWNGRADING SCHEDULE |

16. DISTRIBUTION STATEMENT (of this Report)

APPROVED FOR PUBLIC RELEASE; DISTRIBUTION UNLIMITED

17. DISTRIBUTION STATEMENT (of the abstract entered in Block 20, if different from Report)

18. SUPPLEMENTARY NOTES

APPROVED FOR PUBLIC RELEASE: IAW AFR 190-1

LYNN E. WOLAVER 7 Apr 86
Dean for Research and
Professional Development
AFIT/NR, WPAFB OH 45433-6583

19. KEY WORDS (Continue on reverse side if necessary and identify by block number)

20. ABSTRACT (Continue on reverse side if necessary and identify by block number)



86 4 [illegible] 073

DD FORM 1 JAN 73 1473 EDITION OF 1 NOV 65 IS OBSOLETE

SECURITY CLASSIFICATION OF THIS PAGE (When Data Entered)

# ABSTRACT

The Effect of Smoothing the Doppler Radar Derived Wind Field on Perturbation Pressure Retrieval. (May 1986)

George Philip Rosser, Jr., B.S., University of Georgia

Chairman of Advisory Committee: Dr. Phanindramohan Das

Gridded u and v wind components derived from dual-Doppler radar data were utilized to study the behavior of the perturbation pressure field when different amounts of smoothing were applied to the wind field. Data-void areas in the wind field were filled by extrapolation. Three-point and nine-point smoothing operators were employed to smooth the wind field prior to retrieving the perturbation pressure field. Smoothing the wind field produced a nonlinear variation of the central pressure value in a meso-low with respect to the smoothing parameter. The central pressure value decreased as the smoothing parameter increased. Pressure centers less than 0.1 kPa (1 mb) in absolute magnitude tended to amplify and migrate slightly. False pressure centers created by the data-void filling technique were removed when a smoothing parameter greater than or equal to 0.4 was employed. Smoothing parameters greater than or equal to 0.5 created a false pressure center.



A-1

# AFIT RESEARCH ASSESSMENT

The purpose of this questionnaire is to ascertain the value and/or contribution of research accomplished by students or faculty of the Air Force Institute of Technology (AU). It would be greatly appreciated if you would complete the following questionnaire and return it to:

AFIT/NR
Wright-Patterson AFB OH 45433

RESEARCH TITLE: _____

_____

AUTHOR: _____

RESEARCH ASSESSMENT QUESTIONS:

1. Did this research contribute to a current Air Force project?

( ) a. YES ( ) b. NO

2. Do you believe this research topic is significant enough that it would have been researched (or contracted) by your organization or another agency if AFIT had not?

( ) a. YES ( ) b. NO

3. The benefits of AFIT research can often be expressed by the equivalent value that your agency achieved/received by virtue of AFIT performing the research. Can you estimate what this research would have cost if it had been accomplished under contract or if it had been done in-house in terms of manpower and/or dollars?

( ) a. MAN-YEARS _____ ( ) b. $_____

4. Often it is not possible to attach equivalent dollar values to research, although the results of the research may, in fact, be important. Whether or not you were able to establish an equivalent value for this research (3. above), what is your estimate of its significance?

( ) a. HIGHLY SIGNIFICANT ( ) b. SIGNIFICANT ( ) c. SLIGHTLY SIGNIFICANT ( ) d. OF NO SIGNIFICANCE

5. AFIT welcomes any further comments you may have on the above questions, or any additional details concerning the current application, future potential, or other value of this research. Please use the bottom part of this questionnaire for your statement(s).

NAME GRADE POSITION

ORGANIZATION LOCATION

STATEMENT(s):

# THE EFFECT OF SMOOTHING THE DOPPLER RADAR DERIVED WIND FIELD ON PERTURBATION PRESSURE RETRIEVAL

A Thesis

by

GEORGE PHILIP ROSSER, JR.

Submitted to the Graduate College of
Texas A&M University
in partial fulfillment of the requirements for the degree of

MASTER OF SCIENCE

May 1986

Major Subject: Meteorology

# THE EFFECT OF SMOOTHING THE DOPPLER RADAR DERIVED WIND FIELD ON PERTURBATION PRESSURE RETRIEVAL

A Thesis

by

GEORGE PHILIP ROSSER, JR.

Submitted to the Graduate College of
Texas A&M University
in partial fulfillment of the requirements for the degree of

MASTER OF SCIENCE

May 1986

Major Subject: Meteorology

# THE EFFECT OF SMOOTHING THE DOPPLER RADAR DERIVED WIND FIELD ON PERTURBATION PRESSURE RETRIEVAL

A Thesis

by

GEORGE PHILIP ROSSER, JR.

Approved as to style and content by:

Phanindramohan Das
Phanindramohan Das
(Chairman of Committee)

Kenneth C. Brundidge
Kenneth C. Brundidge
(Member)

Donald K. Friesen
Donald K. Friesen
(Member)

James R. Scoggins
James R. Scoggins
(Head of Department)

May 1986

# ABSTRACT

The Effect of Smoothing the Doppler Radar Derived Wind Field on Perturbation Pressure Retrieval. (May 1986)

George Philip Rosser, Jr., B.S., University of Georgia

Chairman of Advisory Committee: Dr. Phanindramohan Das

Gridded u and v wind components derived from dual-Doppler radar data were utilized to study the behavior of the perturbation pressure field when different amounts of smoothing were applied to the wind field. Data-void areas in the wind field were filled by extrapolation. Three-point and nine-point smoothing operators were employed to smooth the wind field prior to retrieving the perturbation pressure field. Smoothing the wind field produced a nonlinear variation of the central pressure value in a meso-low with respect to the smoothing parameter. The central pressure value decreased as the smoothing parameter increased. Pressure centers less than 0.1 kPa (1 mb) in absolute magnitude tended to amplify and migrate slightly. False pressure centers created by the data-void filling technique were removed when a smoothing parameter greater than or equal to 0.4 was employed. Smoothing parameters greater than or equal to 0.5 created a false pressure center.

## DEDICATION

This thesis is dedicated to my wife, Chon, and son, George III, whose love, strength, and support give me encouragement and purpose in life. To my sister and brother, Lynn Rosser Allen and James Rosser, whose love and support kept me going. To my father, George P. Rosser, who instilled in me the desire to learn.

# ACKNOWLEDGMENTS

The author would like to express deep gratitude to his committee for their help, support, and guidance. I would like to especially thank Dr. Phanindramohan Das for guidance, tolerance, intellectual stimulation, acquiring the data, and for teaching me to think on my own. I would also like to thank Dr. Kenneth Brundidge for his guidance, comments, and assistance with the preparation of this thesis. Special thanks go to Dr. James Scoggins for making available the Department of Meteorology's computer and graphics resources. Thanks is also extended to Dr. Donald Friesen for reviewing this thesis.

Gratitude is also expressed to the U.S. Air Force and Air Force Institute of Technology for allowing me to attend graduate school at Texas A&M University.

Appreciation and thanks are extended to my friends Major Dave Bonewitz, Captains Danny Pophin, Jill Schmidt, Mike Walters, and Mark Welshinger for their support and help with my graduate studies and course work at Texas A&M University.

# TABLE OF CONTENTS

# LIST OF FIGURES

# 1. INTRODUCTION

The operational meteorologist is given the responsibility to inform the general public of imminent severe weather (e.g., tornadoes, flash floods, severe thunderstorms, damaging winds, damaging hail). Since its inception, the conventional weather radar has been the meteorologist's primary tool for detecting and monitoring severe weather phenomena. However, it has certain limitations. The conventional weather radar is only capable of representing the spatial distribution, continuity of movement, and intensity of the precipitation echoes relative to severe weather phenomena. It is incapable of depicting storm kinematics, dynamics, or thermodynamics. The availability of some of this information might improve the timely issuance of weather warnings to the public, decrease false alarms by improving the accuracy of warnings, or provide insight into the nature and behavior of phenomena peculiar to convective storm activity. Part of this information is now available from Doppler radars.

With the advent of the Doppler radar, meteorologists are now able to examine the internal kinematics of convective storms. Single and multiple-Doppler radars provide velocity data from which the internal kinematic structure is readily obtained. In recent years, it has been found feasible to obtain information on the thermodynamics and dynamics of convective phenomena through the use of the four-dimensional velocity information obtained from the Doppler radar by solving the relevant dynamical equations.

---

The citations on the following pages follows the style of the Journal of the Atmospheric Sciences.

In seeking dynamic and thermodynamic information from Doppler data, particular attention has been given to the tornadic thunderstorm and significant insight has been obtained on their dynamic structure. Since the method of retrieving dynamical information from kinematic data promises to be a powerful tool in our analysis of convective storms, we need to carefully analyze the implication of the numerical methods used in such retrieval. One serious problem appears to be the noise in whatever wind data are available. This problem is compounded by the presence of data-void regions due to the absence of adequate precipitation, which need to be filled by some extrapolation or interpolation procedure which itself can be a source of noise. In order to circumvent the noise problem, some kind of smoothing scheme is applied to the wind data before they are used in the retrieval scheme.

This study will examine the role of smoothing on the retrieved perturbation pressure field obtained from the dual-Doppler radar data.

## 2. BACKGROUND

In the late 1970's, as indicated above, the retrieval of thermodynamic information from Doppler radar was demonstrated to be feasible. Initial research by Bonesteele and Lin (1978), Hane and Scott (1978), and Gal-Chen (1978) showed that the kinematic information from Doppler radar could be used in the dynamical equations to deduce the pressure distribution associated with the wind field.

Bonestelle and Lin (1978) worked with actual storm data. They combined two different sets of single-Doppler radar data from two tornadic thunderstorms having similar characteristics to build one composite storm. The temperature distribution was specified around the boundary of the computational domain, and the (horizontal) perturbation pressure field was then retrieved from the composite data set. In their retrieval scheme, they assumed the storm to be in the steady state. Their results indicated that perturbation pressure forces were important for accelerating moist flow toward the updraft and then upward into it, while these forces decelerated the downdraft in the area of the meso-high and induced updrafts along the gust front.

Hane and Scott (1978) and Gal-Chen (1978) employed synthetic data generated from convective cloud models to test their retrieval schemes. Gal-Chen (1978) introduced pseudo-random noise into the test data to determine how it affected the retrieved thermodynamic fields (perturbation pressure and temperature). In both cases, the steady state assumption was examined and found to be partially invalid.

Research conducted during the early 1980's (Clark *et al.*, 1980; Hane *et al.*, 1980) continued the focus on the error caused when

different levels of noise are introduced into the synthetic data. Time evolution, advection, sampling time, and pseudo-random errors (noise) were evaluated by simulating radar data collection through convective cloud models. The thermodynamic retrieval schemes were found to be sensitive to the sampling time (frequency of observations) and white noise. These analyses point up the question, already asked by Hane and Scott (1978), namely, whether a filtering of Doppler-radar data sufficient to suppress unrepresentative noise will still allow the calculation of meaningful results. Another problem, related to using observed data with retrieval schemes, was identified by Hane and Scott (1978). It involved the filling of data voids. The computational schemes require velocity information at every grid point in a three-dimensional Cartesian domain, whereas observed data will only be available within irregular boundaries. They also noted that care should be exercised when interfacing environmental data with Doppler data.

Gal-Chen (1978) experimented with a linear smoothing operator to filter noise. From Doppler radar experiments, conducted in the planetary boundary layer to determine heat and momentum fluxes, Gal-Chen and Kropfli (1984) found that a "more accurate pressure field" resulted if the velocity field is smoothed prior to the retrieval of the pressure and temperature perturbations. Brandes (1984b) also applied a smoothing scheme to the Doppler radar-derived velocity field prior to retrieving pressure and buoyancy perturbations.

With it being apparent that some form of smoothing is necessary, the effort of this study will be to examine the behavior of the perturbation pressure field when different amounts of smoothing are applied to the Doppler radar-derived wind field.

## 3. THEORY

As mentioned above, retrieval of thermodynamic information from Doppler radars was realized in the late 1970's. The retrieval procedure in this study is based on the horizontal momentum equations and the anelastic continuity equation (Pasken and Lin, 1982). Because it is convenient to use a rectangular computational domain, data voids adjacent to the observed data are filled via an objective analysis technique. Since the data generated to fill in the data-void areas are fictitious, a smoothing scheme is necessary to decrease excessive gradients generated in the vicinity of such data (Brandes, 1984a).

### a. Perturbation pressure retrieval scheme

For retrieval of the perturbation pressure, the assumption of a hydrostatic, adiabatic base-state atmosphere is easily justified. In addition, the governing equations can be simplified through the anelastic approximation (Ogura and Phillips, 1962). Two additional assumptions, that of a steady state and a frictionless atmosphere, while generally invalid, are imposed for simplicity. It may be noted that the study being reported has rather limited objectives, and these assumptions do not detract from these objectives.

With the above assumptions, the governing (quasi-horizontal) equations are as follows:

$$\vec{C}\cdot\nabla u = -\frac{1}{\rho_e}\frac{\partial p}{\partial x} + f_o v \ , \qquad (1)$$

$$\vec{C}\cdot\nabla v = -\frac{1}{\rho_e}\frac{\partial p}{\partial y} - f_o u \ , \tag{2}$$

$$\nabla\cdot(\rho_e\vec{C}) = 0 \ , \tag{3}$$

$$p = p_e + p' \ , \tag{4}$$

where $\vec{C}$ is the three-dimensional velocity vector, u and v are the x and y components of the horizontal velocity, respectively, p is the total pressure, $p_e$ is the environmental hydrostatic pressure, p' is the perturbation pressure, $f_o$ is the constant Coriolis parameter, $\nabla$ is the three-dimensional gradient operator, and $\rho_e$ is the environmental density which is a function of height only.

Following the method of Pasken and Lin (1982), (1) and (2) are put in the flux form as follows:

$$\frac{\partial p}{\partial x} = -\frac{\partial(\rho_e uu)}{\partial x} - \frac{\partial(\rho_e vu)}{\partial y} - \frac{\partial(\rho_e wu)}{\partial z} + \rho_e f_o v \ , \tag{5}$$

$$\frac{\partial p}{\partial y} = -\frac{\partial(\rho_e uv)}{\partial x} - \frac{\partial(\rho_e vv)}{\partial y} - \frac{\partial(\rho_e wv)}{\partial z} - \rho_e f_o u \ . \tag{6}$$

By taking the first derivatives with respect to x and y of (5) and (6), respectively, and then adding them together, the following Poisson equation for perturbation pressure is obtained:

$$\nabla_2^2 p' = \rho_e f_o\left(\frac{\partial v}{\partial x} - \frac{\partial u}{\partial y}\right) - \left(\frac{\partial^2(\rho_e u^2)}{\partial x^2} + 2\,\frac{\partial^2(\rho_e uv)}{\partial x \partial y} + \frac{\partial^2(\rho_e v^2)}{\partial y^2}\right)$$

(Cont.)

$$- \frac{\partial^2(u\rho_e w)}{\partial x \partial z} - \frac{\partial^2(v\rho_e w)}{\partial y \partial z} , \qquad (7)$$

where $\nabla_2^2$ is the (horizontal) two-dimensional Laplacian operator. Since the domain used is too small to be free from the effect of the storm, the lateral boundary conditions imposed are of the Neumann type, namely:

$$\frac{\partial p'}{\partial x} = - \rho_e \vec{C} \cdot \nabla u + \rho_e f_o v , \qquad (8)$$

and

$$\frac{\partial p'}{\partial y} = - \rho_e \vec{C} \cdot \nabla v - \rho_e f_o u . \qquad (9)$$

Since u and v wind components are available from Doppler radar, the vertical mass flux per unit area can be obtained from (3) with no-slip surface condition. Perturbation pressure can then be obtained from (7) with boundary conditions (8) and (9) since the forcing terms in (7) are known functions of position. It may be noted that the Coriolis terms could be scaled out of the momentum equations, but they are retained since the resulting increase in complexity is small. It is important to note that three dimensionality enters into these equations through the vertical advection terms.

b. Objective analysis for filling of data-void regions

A weighted mean recursive interpolation scheme was used to estimate grid point values of u and v wind components in the data-void regions (Cressman, 1960; and Trares and Das, 1982). This method of objective analysis represents a quantity at a grid point as the sum of the weighted values of data, within a specified radius of influence, surrounding

the quantity to be interpolated. With this procedure, values are extrapolated and interpolated into the data-void areas by two successive applications of this scheme. A 10 km radius of influence was used. The weight function is dependent on the influence radius and the distance between grid points (resolution).

The interpolated quantity at a grid point is defined as follows:

$$\bar{q}(x,y) = \sum_{m=1}^{M} \xi(d,r)q(x,y) \; / \; \sum_{m=1}^{M} \xi(d,r) \; , \tag{10}$$

where x and y are the Cartesian coordinates of a grid point, r is the radius of influence, d is the distance between the interpolated quantity ($\bar{q}$) and the weighted quantity (q), M is the number of points within the radius of influence, and $\xi$ is the weight function. The particular weight function employed is that devised by Barnes (1964). It is defined as follows:

$$\xi(d,r) = \exp(-4d^2/r^2) \; , \tag{11}$$

where 4 represents a reliability factor related to the ability of the weight function to represent the influence of the data within the radius of influence. As with any weighted mean interpolation scheme, a certain degree of smoothing is present (Barnes, 1964; Trares and Das, 1982).

c. Smoothing scheme

Three-point and nine-point smoothing operators were employed to examine how different amounts of smoothing of the wind field affected the perturbation pressure field. The (one-dimensional) three-point operator

is defined as follows:

$$\bar{G}_i = (1-\sigma)G_i + \frac{\sigma}{2}(G_{i+1} + G_{i-1}) \ . \tag{12}$$

Application of this operator in two dimensions (or directions) gives the nine-point smoothing operator

$$\begin{aligned}\bar{G}^{ij}_{i,j} &= (1-\sigma)^2 G_{i,j} + \sigma(1-\sigma)(G_{i+1,j} + G_{i-1,j} + G_{i,j+1} + G_{i,j-1})/2 \\ &\quad + \sigma^2 (G_{i+1,j+1} + G_{i-1,j+1} + G_{i+1,j-1} + G_{i-1,j-1})/4 \\ &= RG_{i,j} \ ,\end{aligned} \tag{13}$$

where i and j represent coordinates of a grid point, $G_{i,j}$ is the original value of the quantity to be smoothed, $\bar{G}^{ij}_{i,j}$ represents the smoothed quantity, ij superscript means smoothing in the x-direction then in the y-direction with the (one-dimensional) three-point operator (12), $\sigma$ is the smoothing parameter, and R is the response function.

If the spatial distribution of a variable can be represented as a harmonic function, then the response function obtained by inserting a simple harmonic function of the form

$$G(x,y) = A\exp(i(kx + \ell y)) \ , \tag{14}$$

into (13) gives a response function of

$$R = (1 - 2\sigma\sin^2(\frac{k\Delta x}{2})) * (1 - 2\sigma\sin^2(\frac{\ell\Delta y}{2})) \ , \tag{15}$$

where A represents the wave amplitude, $\Delta x$ and $\Delta y$ are the grid distances

in the x and y directions, respectively, and k and $\ell$ are the wave numbers in the x and y directions, respectively. For smoothing parameters less than or equal to 0.5, the smoothing schemes do not affect the wave number or the phase of the original wave, and are independent of the first direction smoothed. With a smoothing parameter greater than 0.5, the one-dimensional smoothing operator will produce a phase shift and the two-dimensional smoothing operator will allow shortwave noise to appear. Fig. 1 is a graph of the response function (R) for different values of the smoothing parameter with $k = 2\pi/\lambda$ and $\Delta x = \Delta y = d$. For $\sigma = 0.5$ and $\lambda = 11d$, the response function is $R = 0.85$. This means that a wave with a wavelength of 11d will lose only 15% of its amplitude when smoothed. On the other hand, for the same smoothing parameter, a wave with a wavelength of $\lambda = 2d$ will be completely removed (Shuman, 1958; Haltiner and Williams, 1980).

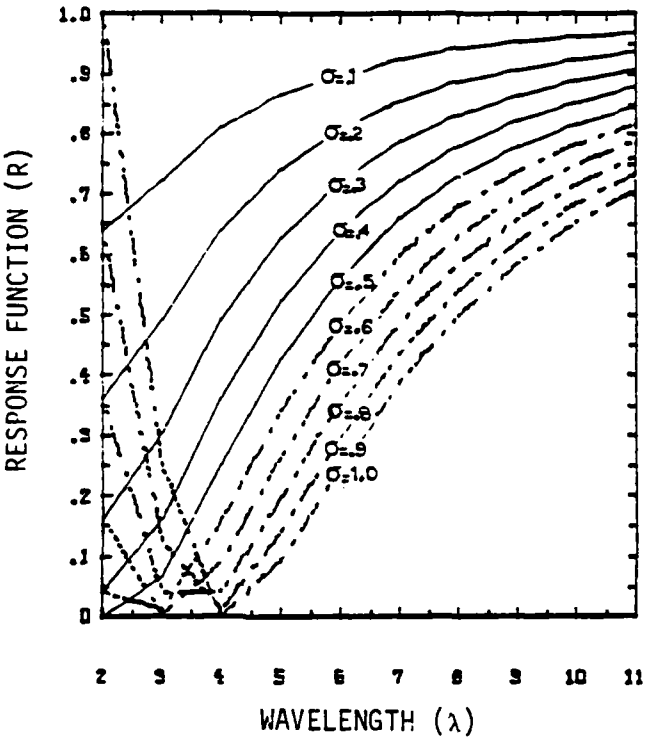


Fig. 1. The response function versus wavelength for different smoothing parameters. Wavelength is multiples of the grid spacing (d).

## 4. NUMERICAL METHODS

### a. Numerical grid

The numerical work is performed on a standard three-dimensional Cartesian grid. The points are spaced evenly every 1000 m in the horizontal and vertical directions. Only two vertical levels above the surface are considered since the study is more for examining the soundness of the methodology than for unravelling storm characteristics.

In the difference equations presented below, the grid intervals are $\Delta x = \Delta y = \Delta z = d$ (= 1000 m). The customary indices i and j are used for the grid points in the x- and y-directions, respectively, and the subscript n is used to indicate vertical levels.

### b. Finite-difference equations

(i) Anelastic Continuity Equation. The vertical mass flux per unit area was obtained by vertical integration of the anelastic continuity equation (3) in finite-difference form as follows:

$$(\rho_e w)_{n+1} = (\rho_e w)_n$$

$$- (((\rho_e u_{i+1,j,n} - \rho_e u_{i-1,j,n} + \rho_e u_{i+1,j,n+1} - \rho_e u_{i-1,j,n+1})/2d$$

$$+ \rho_e v_{i,j+1,n} - \rho_e v_{i,j-1,n} + \rho_e v_{i,j+1,n+1} - \rho_e v_{i,j-1,n+1})/2d)/2)*d \quad (16)$$

The vertical mass flux was computed at the first two vertical levels above the bottom boundary of the computational domain. It may be noted that a trapezoidal form is used in the vertical with a centered difference in the horizontal. Vertical velocity is treated as zero at the

lower boundary.

(ii) Perturbation Pressure. Equation (9) is put in finite-difference form as follows:

$$P_{i+1,j} + P_{i-1,j} + P_{i,j+1} + P_{i,j-1} - 4*P_{i,j}$$

$$= \rho_e*f_o*((v_{i+1,j} - v_{i-1,j})/2d - (u_{i,j+1} - u_{i,j-1})/2d$$

$$- \rho_e*((u^2_{i+1,j} - 2*u^2_{i,j} + u^2_{i-1,j})/d^2$$

$$+ 2*((uv)_{i+1,j+1} - (uv)_{i+1,j-1} - (uv)_{i-1,j+1} + (uv)_{i-1,j-1})/d^2$$

$$+ (v^2_{i,j+1} - 2*v^2_{i,j} + v^2_{i,j-1})d^2)$$

$$- ((u\rho_e w)_{i+1,n+1} - (u\rho_e w)_{i+1,n-1} - (u\rho_e w)_{i-1,n+1} + (u\rho_e w)_{i-1,n-1})/d^2$$

$$- ((v\rho_e w)_{j+1,n+1} - (v\rho_e w)_{j+1,n-1} - (v\rho_e w)_{j-1,n+1} + (v\rho_e w)_{j-1,n-1})/d^2 \qquad (17)$$

where P represents the perturbation pressure in the above finite-difference formula.

(iii) Poisson Solver. The alternating direction implicit method is employed to solve (17) which is put into an implicit-iteration scheme as follows:

$$P^{t+1}_{i,j} = P^t_{i,j} + \beta*(P_{i+1,j} - 2*P_{i,j} + P_{i-1,j})^{t+1}$$

$$+ \beta*(P_{i,j+1} - 2*P_{i,j} + P_{i,j-1})^t - d^2*H_{i,j}*\beta \quad , \qquad (18)$$

$$P_{i,j}^{t+2} = P_{i,j}^{t+1} + \beta*(P_{i+1,j} - 2*P_{i,j} + P_{i-1,j})^{t+1}$$

$$+ \beta*(P_{i,j+1} - 2*P_{i,j} + P_{i,j-1})^{t+2} - d^2*H_{i,j}*\beta \ , \qquad (19)$$

where $\beta$ is an acceleration parameter, t is an iteration level, and $H_{i,j}$ (forcing function) represents the right-hand side of (7). Equation (18) is solved for the rows of the numerical grid and (19) is solved for the columns of the numerical grid using the solution obtained from (18). Equation (18) is again solved with information obtained from (19). This numerical procedure is repeated until a desired level of tolerance is obtained. All terms in this scheme and in the forcing function are computed via standard centered differences (Gerald and Wheatly, 1984).

## 5. DATA AND PROCEDURE

### a. Data

Dual-Doppler radar data used in this study were collected by the National Severe Storms Laboratory (NSSL) on 2 May during project SESAME (Severe Environmental Storms And Mesoscale Experiment) conducted in 1979. NSSL and its corresponding network of Doppler radars are located in Oklahoma.

On the morning of 2 May 1979, synoptic charts indicated the probability of further thunderstorm development from pre-existing nocturnal thunderstorm activity in Oklahoma. The stability indices, vertical wind shear, frontal position, and approaching 50 kPa short wave trough were conducive for possible severe thunderstorm development during the next 24 h. By mid-afternoon, isolated thunderstorm activity developed about 175 km northwest of Norman, Oklahoma. The thunderstorm activity intensified, and two large cells spawned tornadoes. Doppler-radar data collection began around 1630 LST. The data used in this study were collected at 1651 LST (Alberty *et al.*, 1979).

The basic data used in this study are the u and v wind components and density taken from a vertical sounding. One section of a line of tornadic thunderstorms associated with a meso-circulation was examined in this study. The wind component data have already been assigned to a Cartesian grid spaced at 1000 m intervals in the horizontal and vertical directions. The sounding data have already been assigned to 1000 m intervals in the vertical direction. Fig. 2 is a display of the gridded wind field, derived from dual-Doppler radars, which includes general data-void areas.

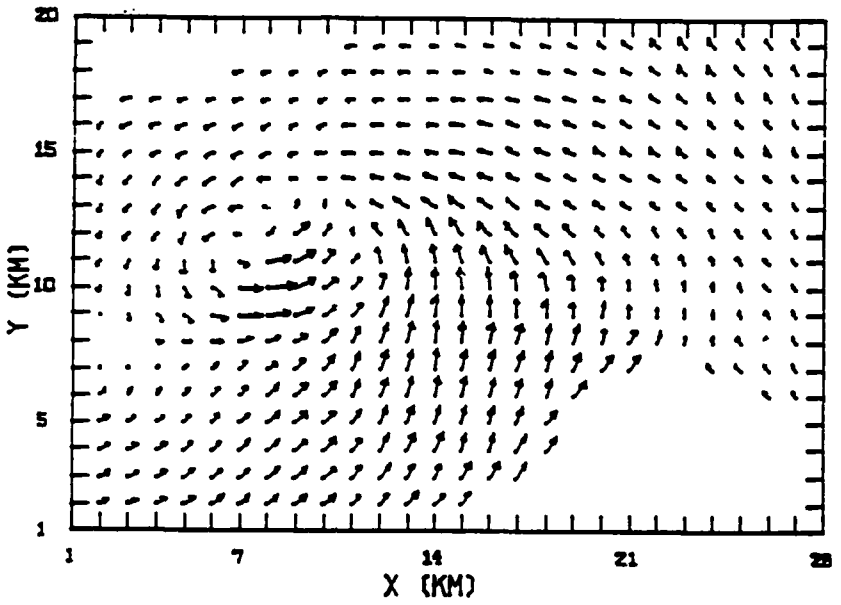


Fig. 2. Gridded wind field derived from dual-Doppler radars. A wind vector 0.45 cm in length represents a velocity of 50 $ms^{-1}$.

As can be seen in Fig. 2, the samples of velocity data from dual-Doppler radars have some inherent problems, one of which is that information is only available within irregular boundaries. In addition, the velocity measurements are contaminated by a considerable amount of noise with typical errors of 1-3 $ms^{-1}$ or more in areas of low signal intensity. Other possible problems exist with the data used in this study, namely, those due to the location of storms from the radars (40-115 km), which impact on the resolution of low-level phenomena and small-scale features (Brandes, 1984b). Fortunately, these do not seriously affect the present study.

The nature of the storms and data collection presents wind information contained within irregular boundaries. To avoid an irregular computation domain and for convenience, data-void areas in the observed wind field were filled prior to the retrieval of the perturbation pressure. The data-void filling procedure was applied to minimize forcing (i.e., excessive gradients) between areas with data and areas without data so that a rectangular computational domain could be used. All data voids in the wind field were filled by extrapolating and interpolating values into the data-void regions.

b. Smoothing

The theory and properties of the smoothing operator were discussed in Chapter 3. The three-point and nine-point smoothing operators are utilized to smooth the Doppler derived wind field prior to retrieving the perturbation pressure. This was done to suppress noise, to suppress discontinuities generated by the data-void filling procedure, and primarily to study the response of the perturbation pressure field to the

smoothing of the wind field.

The boundary winds are smoothed with the three-point smoothing operator, and the rest of the wind field is smoothed with the nine-point smoothing operator.

Different amounts of smoothing were applied to the wind field, after the filling of the data voids and prior to retrieving the perturbation pressure, to determine how the smoothing influenced the perturbation pressure field. Values of the smoothing parameter used ranged from 0.0 to 1.0 with 0.1 increments.

c. Perturbation pressure retrieval

The scheme for the retrieval of perturbation pressure from dual-Doppler radar derived wind fields has been described earlier. With the u and v wind components available from Doppler radar and density available from a vertical sounding, the vertical mass flux per unit area was obtained from the anelastic continuity equation. This makes the right-hand side of (7) a known function of position so that the Poisson equation for perturbation pressure can be solved.

The particular numerical technique used is the alternating direction implicit (ADI) procedure. In implementing this numerical procedure, (18) is solved by sweeping only the rows of the numerical grid and (19) by sweeping the columns of the numerical grid, using information from (18), to obtain a solution. Equation (18) is again solved with information obtained from (19). This numerical procedure is repeated until the change in the solution, between successive iteration stages, has reached (or become less than) an assigned tolerance which was set at $10^{-5}$. A $\beta = 4.0$ was found to give the fastest convergence for

streamfunction retrieval.

It was found that a convergence criterion smaller than $10^{-5}$ will cause the number of iterations to go from 146 to over 1000 using the ADI scheme when implemented on the Harris 500 computer in the single precision mode. For the problem in hand, the tolerance of $10^{-5}$ was considered adequate.

## 6. RESULTS

The perturbation pressure patterns, associated with different amounts of smoothing applied to the wind field, have been contoured and displayed in Figs. 3-13.

Fig. 3 is the perturbation pressure pattern associated with the unsmoothed wind field. The meso-low (-1.55 kPa) pressure area, located at x = 8 km and y = 11 km, coincides with the meso-circulation seen in Fig. 2; this is in agreement with previous research (Bonesteele and Lin, 1978). The two meso-high pressure centers (0.549 and 0.554 kPa) in Fig. 3 appear to be due to extraneous forcing caused by the data-void filling procedure. There is no evidence in the wind pattern that supports these perturbation high-pressure centers. The broad low pressure area to the southeast of the meso-low pressure center is characteristic of the perturbation pressure pattern associated with meso-circulations; this is also in agreement with previous research (Bonesteele and Lin, 1978).

Figs. 4-13 show how the perturbation pressure field responds to increased smoothing (increase in the value of the smoothing parameter) of the wind field. The false perturbation-high pressure centers are smoothed out except for one located at x = 21 km and y = 8 km. A false pressure center appears after the wind field is smoothed with the use of a smoothing parameter greater than or equal to 0.5. This is evident in Figs. 8-13 at x = 23 km and y = 19 km. This pressure center continues to amplify as the wind field is increasingly smoothed (Figs. 9-13). The two pressure centers located at x = 2 km and y = 8 km and x = 1 km and y = 4 km are amplifying and decaying, respectively, in amplitude as more smoothing is applied to the wind field.

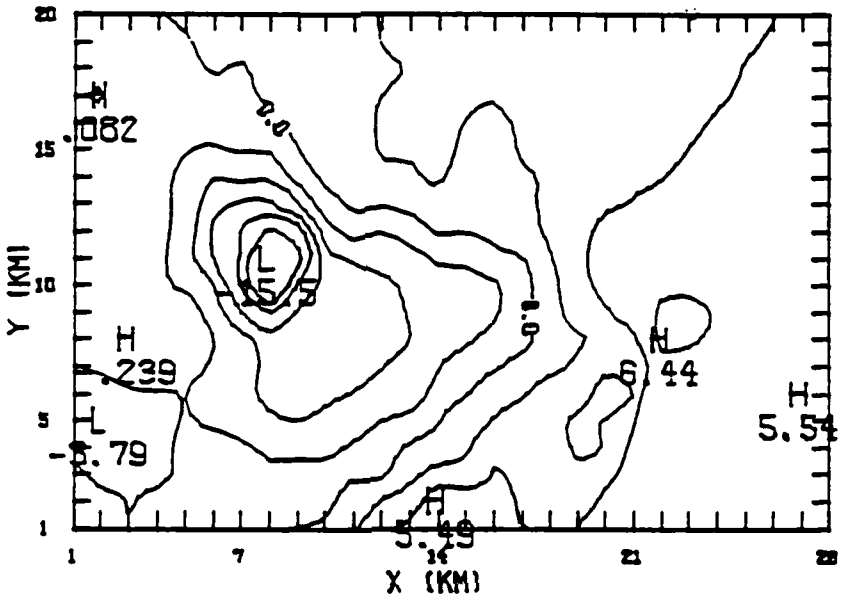


Fig. 3. Perturbation pressure field for an unsmoothed wind field. Units are 0.1 kPa. Contour interval is 0.2 kPa. Relative high and low pressure centers are denoted by H and L, respectively.

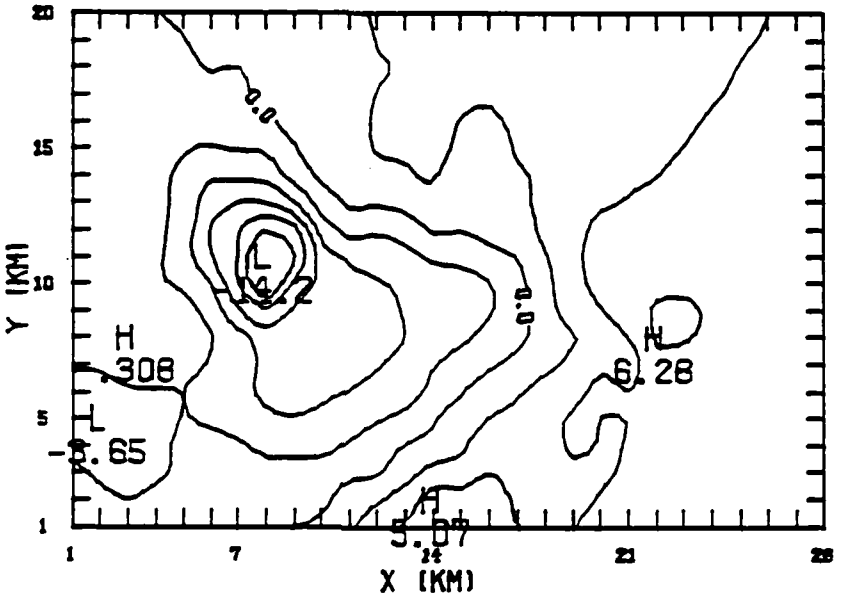


Fig. 4. Perturbation pressure field for $\sigma$ = 0.1. Units are 0.1 kPa. Contour interval is 0.2 kPa.

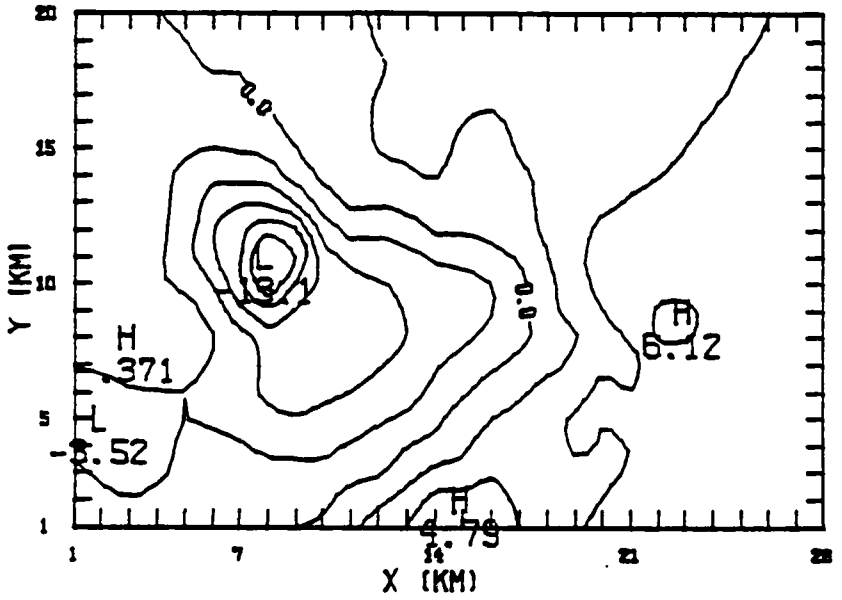


Fig. 5. Perturbation pressure field for $\sigma$ = 0.2. Units are 0.1 kPa. Contour interval is 0.2 kPa.

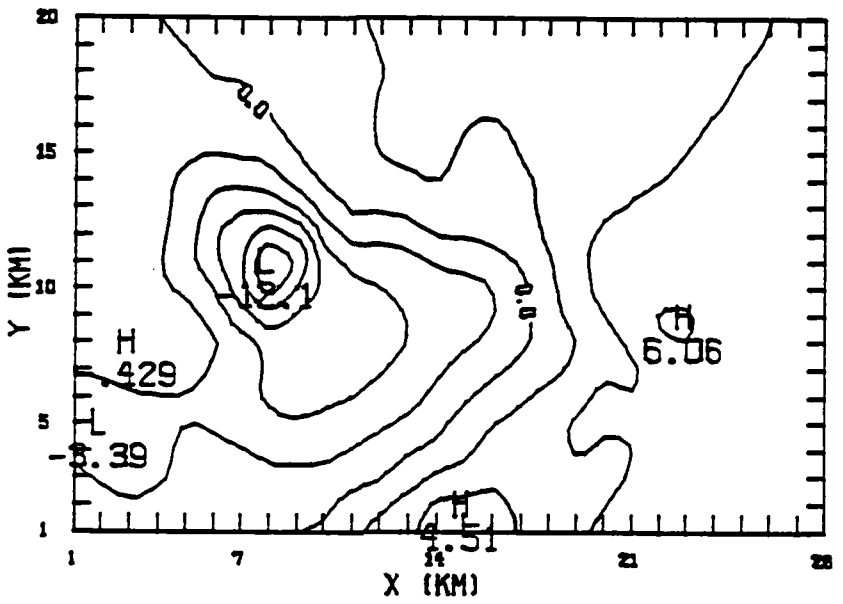


Fig. 6. Perturbation pressure field for $\sigma$ = 0.3. Units are 0.1 kPa. Contour interval is 0.2 kPa.

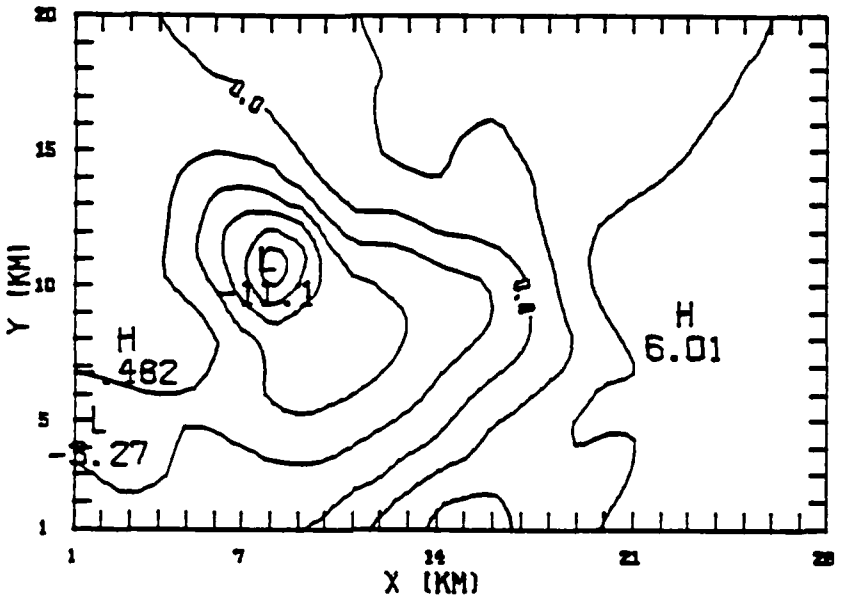


Fig. 7. Perturbation pressure field for $\sigma = 0.4$. Units are 0.1 kPa. Contour interval is 0.2 kPa.

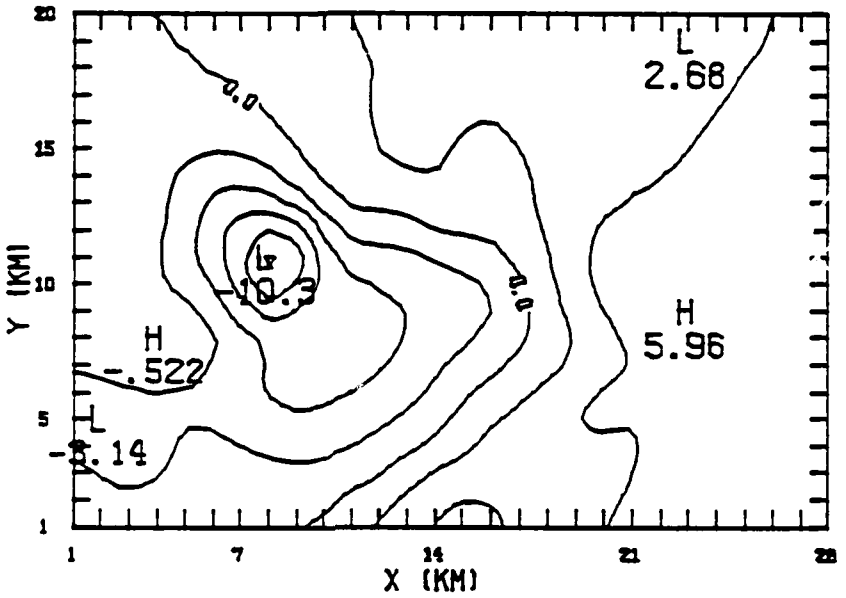


Fig. 8. Perturbation pressure field for $\sigma$ = 0.5. Units are 0.1 kPa. Contour interval is 0.2 kPa.

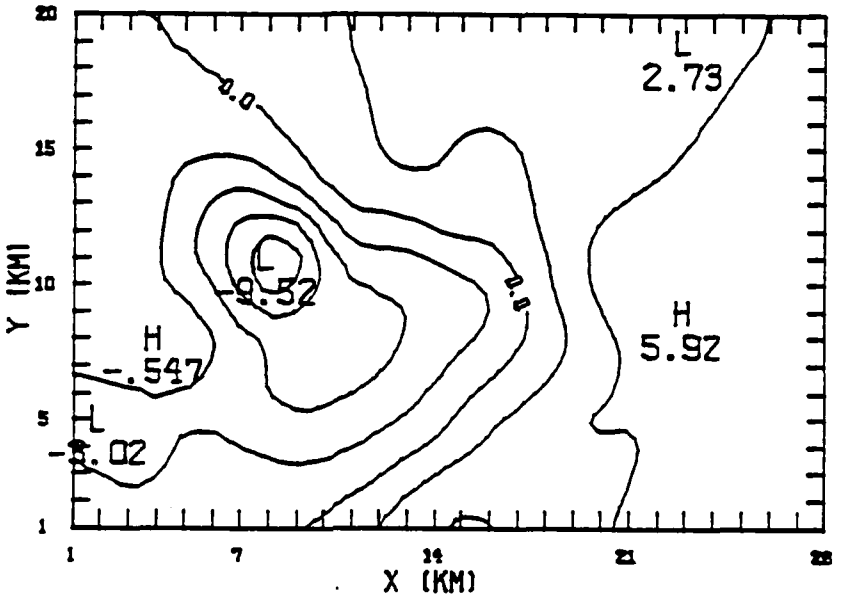


Fig. 9. Perturbation pressure field for $\sigma$ = 0.6. Units are 0.1 kPa. Contour interval is 0.2 kPa.

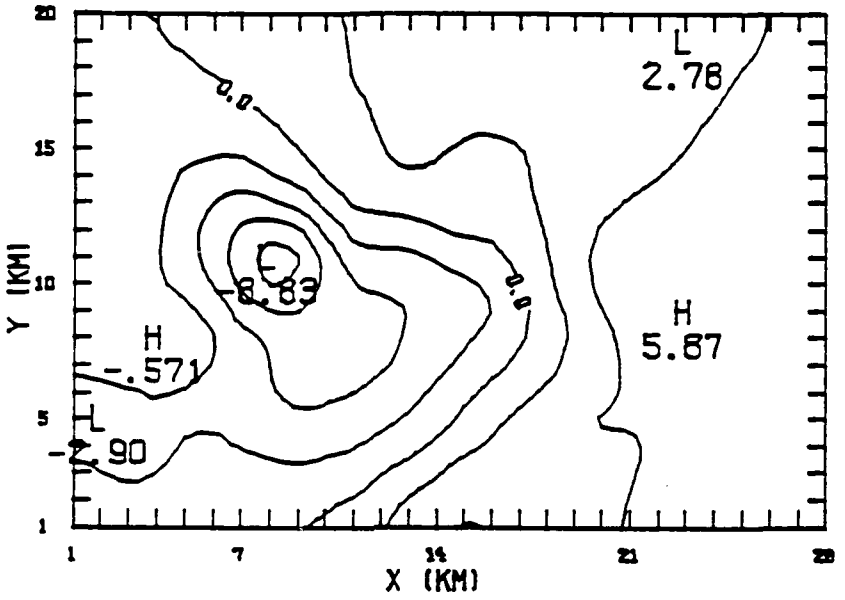


Fig. 10. Perturbation pressure field for $\sigma$ = 0.7. Units are 0.1 kPa. Contour interval is 0.2 kPa.

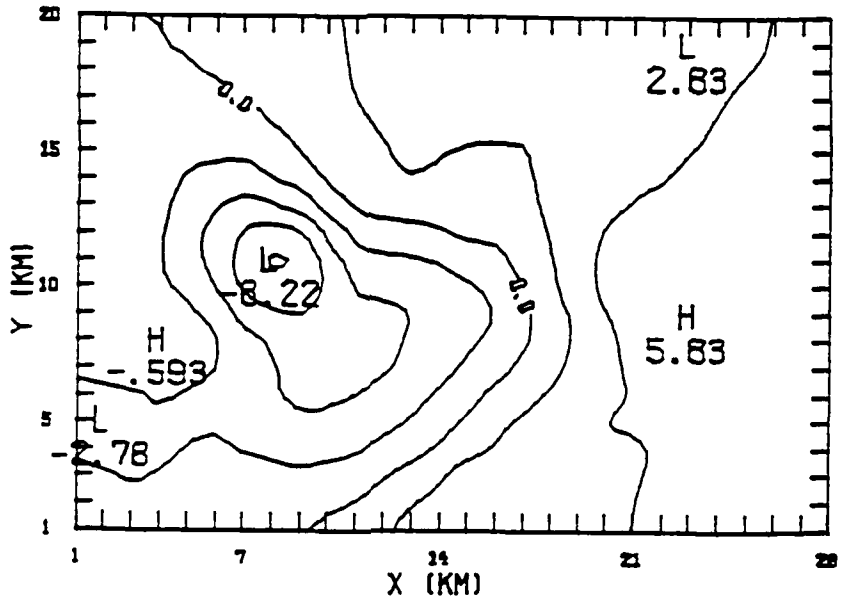


Fig. 11. Perturbation pressure field for $\sigma$ = 0.8. Units are 0.1 kPa. Contour interval is 0.2 kPa.

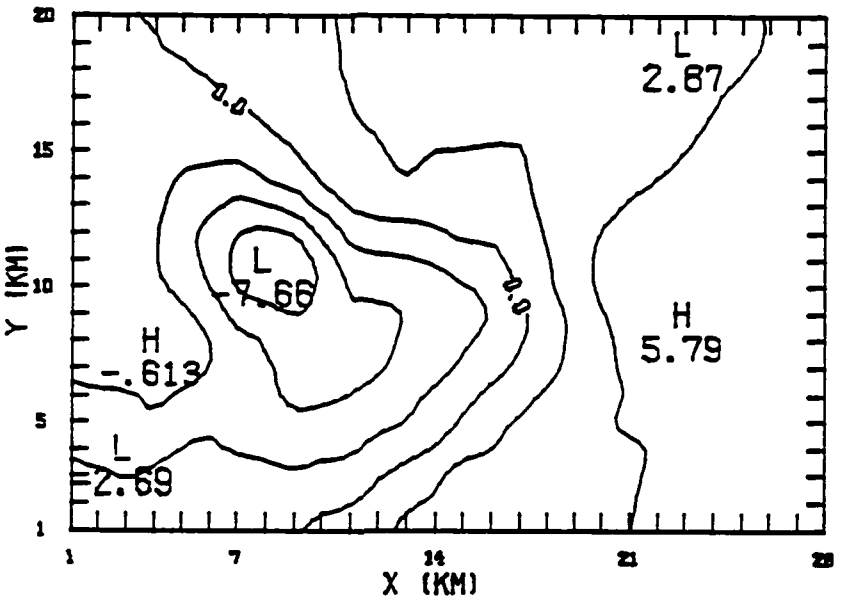


Fig. 12. Perturbation pressure field for $\sigma$ = 0.9. Units are 0.1 kPa. Contour interval is 0.2 kPa.

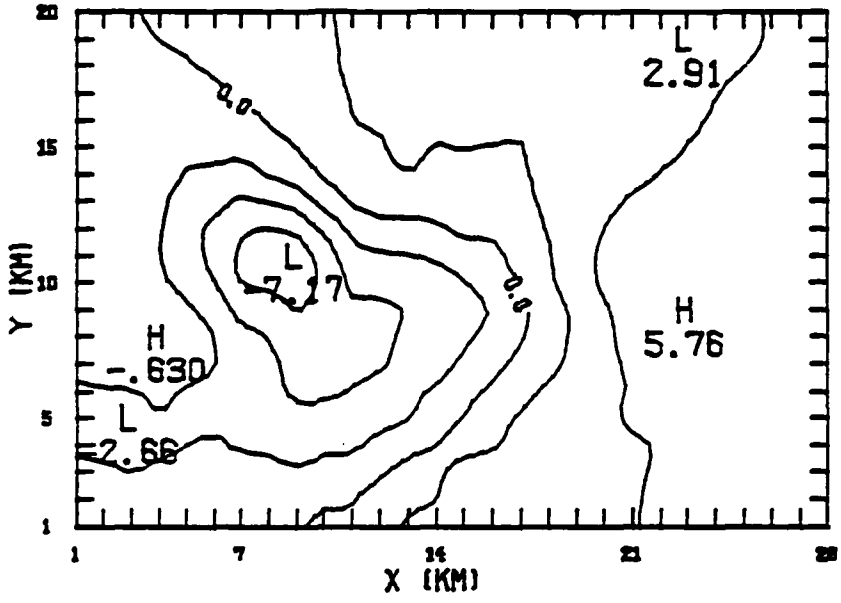


Fig. 13. Perturbation pressure field for $\sigma$ = 1.0. Units are 0.1 kPa. Contour interval is 0.2 kPa.

From examining Figs. 4-13, it is apparent that a smoothing parameter greater than or equal to 0.5 will create a false pressure center and cause the smooth isobar pattern obtained from lighter smoothing to become noisy again. Also, values less than 0.1 kPa (absolute value) tend to amplify and migrate slightly. This is apparent from the pressure value located initially at x = 3 km and y = 8 km in Fig. 3. In Fig. 13, this pressure center has moved to x = 4 km and y = 8 km.

Fig. 14 is a graph of the center pressure value of the meso-low for different values of the smoothing parameter, normalized by the central pressure value obtained from the unsmoothed wind field, plotted against the smoothing parameter. The relationship is nonlinear but appears close to being linear. This may be due to the fact that the smoothing operator is linear whereas the forcing for the perturbation pressure in (7) is nonlinear.

Figs. 15 and 16 are the divergence and vorticity fields associated with the unsmoothed wind field, respectively. Values of divergence and vorticity are in units of $10^{-2}$ $s^{-1}$. An approximate theoretical estimate of vorticity in the meso-low, assumed to be a Rankine vortex, was made to be consistent with the pressure value in the meso-low for the unsmoothed wind (Fig. 3). The value of the vorticity obtained, assuming a radius of 3000 m, is 2.6 x $10^{-2}$ $s^{-1}$. In Fig. 16, the value is 3.9 x $10^{-2}$ $s^{-1}$. The theoretical value for vorticity agrees fairly well with the actual value of vorticity. The difference may be attributed to the divergence field associated with the meso-circulation (Fig. 2 and Fig. 15) since the wind field of the Rankine vortex is non-divergent.

The 0.644 kPa meso-high pressure in Fig. 3, x = 22 km and y = 8 km, has some support from the divergence field displayed in Fig. 15.

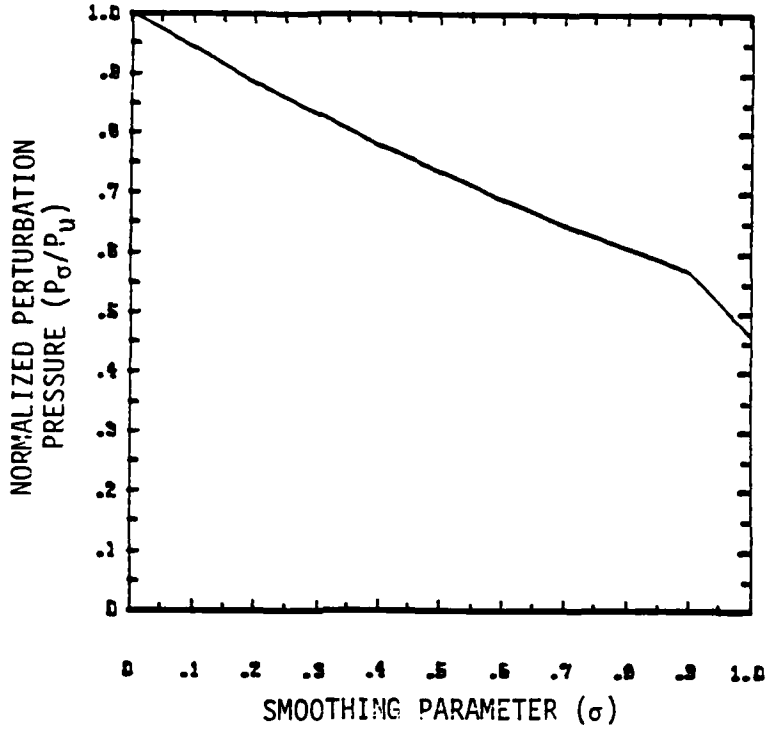


Fig. 14. Effect of smoothing on retrieved perturbation pressure at the center of the principal meso-low. $P_\sigma$ is perturbation pressure obtained with the smoothing parameter ($\sigma$). $P_u$ is perturbation pressure obtained from unsmoothed wind field.

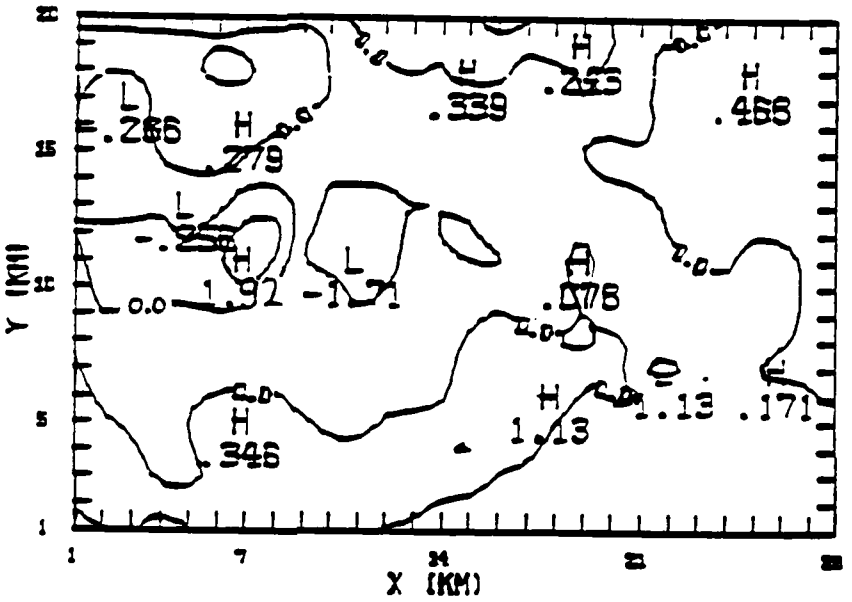


Fig. 15. Divergence field associated with the unsmoothed wind field. Units are $10^{-2}$ $s^{-1}$. Contour interval is $10^{-2}$ $s^{-1}$. Centers of divergence and convergence are denoted by H and L, respectively.

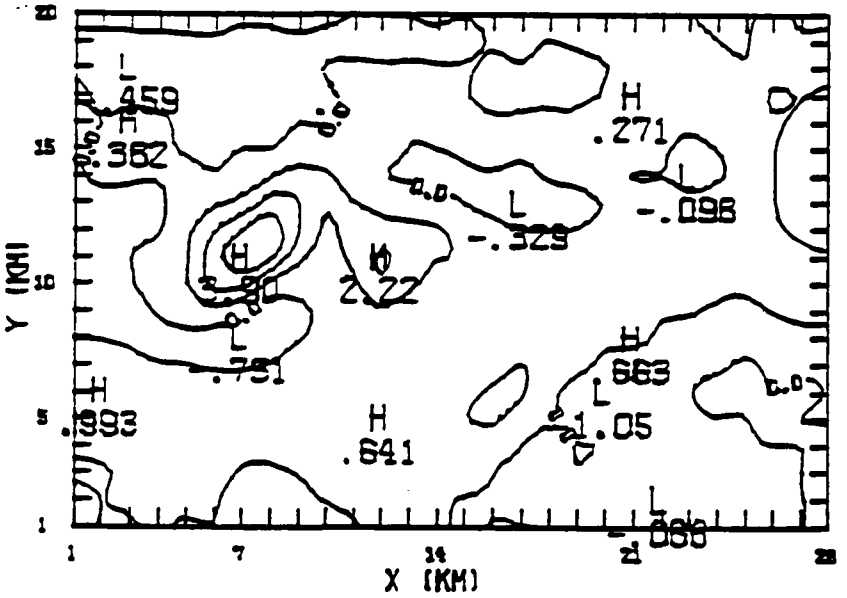


Fig. 16. Vorticity field associated with the unsmoothed wind field. Units are $10^{-2}$ $s^{-1}$. Contour interval is $10^{-2}$ $s^{-1}$. Positive and negative vorticity centers are denoted by H and L, respectively.

However, the divergence value in the general location is very weak.

# 7. CONCLUSIONS AND RECOMMENDATIONS

## a. Conclusions

Smoothing the wind field removes most false pressure centers generated by extraneous forcing from the data-void filling procedure. However, values of the smoothing parameter greater than or equal to 0.5 created a false pressure center. This may be due to the change of phase caused by the three-point smoothing operator used to smooth the boundary winds. Increased smoothing of the wind field caused pressure centers of less than 0.1 kPa (absolute magnitude) to amplify and migrate slightly. A smoothing parameter of 0.4 will remove false pressure centers generated by the data-void filling technique without introducing more short-wave noise. Increased smoothing with a smoothing parameter greater than or equal to 0.5 caused the smooth isobar pattern obtained from lighter smoothing to become noisy again.

Based on the perturbation pressure field, the wind pattern is highly ageostrophic as would be expected by the scale of the storm. In the meso-low, the wind pattern gives the suggestion of cyclostrophic balance. However, since cyclostrophic flow is nondivergent, the flow deviates considerably from cyclostrophic balance because the wind field in the meso-low is divergent.

## b. Recommendations

(i) Steady State. If possible, the steady state assumption should be discarded and the local time derivatives evaluated. However, this requires short radar scan periods over the same volume sample (Hane and Scott, 1978; Hane et al., 1980; Clark et al., 1980; Gal-Chen and

Kropfli, 1984; Das, 1985).

(ii) Inclusion of Friction. A parameterization of friction should be included in the equations since the flow is not inviscid, and kinetic energy dissipation needs to be accounted for in the equations of motion (Das, 1985).

(iii) Three-Dimensional Smoothing and Retrieval. Because the wind field associated with convective phenomena is a three-dimensional entity, the smoothing scheme applied to the wind field and the retrieval of perturbation pressure needs to be accomplished through three-dimensional equations (Das, 1985).

# REFERENCES


Alberty, L. A., D. W. Burgess, C. E. Hane and J. F. Weaver, 1979: Sesame 1979 Operations Summary, U.S. Dept. of Commerce, 253 pp.

Bonesteele, R. G., and Y. J. Lin, 1978: A study of updraft-downdraft interaction based on perturbation pressure and single-Doppler radar data. Mon. Wea. Rev., 106, 62-68.

Barnes, S. L., 1964: A technique for maximizing details in numerical weather map analysis. J. Appl. Meteor., 3, 396-409.

Brandes, E. A., 1984a: Relationships between radar-derived thermodynamic variables and tornadogenesis. Mon. Wea. Rev., 112, 1033-1052.

_____, 1984b: Personal communication.

Clark, T. L., F. I. Harris and C. G. Mohr, 1980: Errors in wind fields derived from multiple-Doppler radars: Random errors and temporal errors associated with advection and evolution. J. Appl. Meteor., 19, 1273-1284.

Cressman, G. P., 1960: An operational objective analysis system. Mon. Wea. Rev., 87, 367-374.

Das, P., 1985: Personal communication.

Gal-Chen, T., 1978: A method for the initialization of the anelastic equations: Implications for matching models with observations. Mon. Wea. Rev., 106, 587-606.

_____, and R. A. Kropfli, 1984: Buoyancy and pressure perturbations derived from dual-Doppler radar observations of the planetary boundary layer: Applications for matching models with observations. J. Atmos. Sci., 41, 3007-3020.

Gerald, C. F., and P. O. Wheatly, 1984: Applied Numerical Analysis, 3rd ed., Addison-Wesley Publishing Company, Inc., 579 pp.

Hane, C. E., and B. C. Scott, 1978: Temperature and pressure perturbations within convective clouds derived from detailed air motion information: Preliminary testing. Mon. Wea. Rev., 106, 654-661.

_____, R. B. Wilhelmson and T. Gal-Chen, 1980: Retrieval of thermodynamic variables within deep convective clouds: Experiments in three dimensions. Mon. Wea. Rev., 109, 564-576.

Haltiner, G. J., and R. T. Williams, 1980: Numerical Prediction And Dynamic Meteorology, 2nd ed., John Wiley & Sons, Inc., 477 pp.

Ogura, Y., and N. A. Phillips, 1962: Scale analysis of deep and shallow convection in the atmosphere. J. Atmos. Sci., 19, 173-179.

Pasken, R., and Y. J. Lin, 1982: Pressure perturbations within a tornadic storm derived from dual-Doppler wind data. 12th Conf. Severe Local Storms, San Antonio, Amer. Meteor. Soc., 257-260.

Shuman, F. G., 1958: Numerican methods in weather prediction: II. Smoothing and filtering. Mon. Wea. Rev., 85, 357-361.

Trares, J. S., and P. Das, 1982: Representation Of The Mesoscale Wind Field Using A Line Integral Technique. Technical Report, TDWR Contract No. 14-00030, 85 pp.

# VITA

George Philip Rosser, Jr. was born in Naha, Okinawa on February 5, 1957. His father is George P. Rosser, who lives in Elverton, Georgia.

After graduating from Elbert County High School in 1975, Mr. Rosser, Jr. attended the University of Georgia and received a B.S. in mathematics. Upon completion of undergraduate school, he entered the Air Force and was sent to Texas A&M University to study the science of meteorology. After three years of forecasting weather for the Air Force, he returned again to Texas A&M University in 1984 for graduate studies in meteorology.

He is married to the former Myong Chon Yun of Songtan City, Korea. They have one son.

His permanent mailing address if 1555 Tallassee Rd., Athens, GA 30606.

This thesis was typed by Mrs. Jacquelyn V. Strong.

END

DTIC

5-86